UNIVERSITY OF BIRMINGHAM
University of Birmingham Research at Birmingham

MLH1 mediates cytoprotective nucleophagy to resist 5-Fluorouracil-induced cell death in colorectal carcinoma

Manzoor, Shaista; Saber-Ayad, Maha; Maghazachi, Azzam A.; Hamid, Qutayba; Muhammad, Jibran Sualeh

DOI:
10.1016/j.neo.2021.12.003

License:
Creative Commons: Attribution-NonCommercial-NoDerivs (CC BY-NC-ND)

Document Version
Publisher's PDF, also known as Version of record

Citation for published version (Harvard):
Manzoor, S, Saber-Ayad, M, Maghazachi, AA, Hamid, Q & Muhammad, JS 2022, 'MLH1 mediates cytoprotective nucleophagy to resist 5-Fluorouracil-induced cell death in colorectal carcinoma', *Neoplasia (United States)*, vol. 24, no. 2, pp. 76-85. https://doi.org/10.1016/j.neo.2021.12.003

Link to publication on Research at Birmingham portal

General rights
Unless a licence is specified above, all rights (including copyright and moral rights) in this document are retained by the authors and/or the copyright holders. The express permission of the copyright holder must be obtained for any use of this material other than for purposes permitted by law.

•Users may freely distribute the URL that is used to identify this publication.
•Users may download and/or print one copy of the publication from the University of Birmingham research portal for the purpose of private study or non-commercial research.
•User may use extracts from the document in line with the concept of 'fair dealing' under the Copyright, Designs and Patents Act 1988 (?)
•Users may not further distribute the material nor use it for the purposes of commercial gain.

Where a licence is displayed above, please note the terms and conditions of the licence govern your use of this document.

When citing, please reference the published version.

Take down policy
While the University of Birmingham exercises care and attention in making items available there are rare occasions when an item has been uploaded in error or has been deemed to be commercially or otherwise sensitive.

If you believe that this is the case for this document, please contact UBIRA@lists.bham.ac.uk providing details and we will remove access to the work immediately and investigate.

Download date: 08. Jul. 2024

NEOPLASIA
www.neoplasia.com
Volume 24 Number 2 February 2022 pp. 76–85

Original Research

MLH1 mediates cytoprotective nucleophagy to resist 5-Fluorouracil-induced cell death in colorectal carcinoma

Shaista Manzoor[a,b]; Maha Saber-Ayad[b,c,*]; Azzam A. Maghazachi[b,c]; Qutayba Hamid[b,c,d]; Jibran Sualeh Muhammad[a,b,*]

[a] Department of Basic Medical Sciences, College of Medicine, University of Sharjah, Sharjah 27272, United Arab Emirates
[b] Research Institute of Medical and Health Sciences, University of Sharjah, Sharjah, United Arab Emirates
[c] Department of Clinical Sciences, College of Medicine, University of Sharjah, Sharjah 27272, United Arab Emirates
[d] Meakins-Christie Laboratories, Research Institute of the McGill University Health Center, Montreal, QC H4A 3J1, Canada

Abstract

Colorectal Cancer (CRC) with Microsatellite instability (MSI) and mutLhomolog-1 (*MLH1*) gene deficiency are less aggressive than *MLH1* proficient cancers. MLH1 is involved in several cellular processes, but its connection with the autophagy-dependent cellular response towards anticancer drugs remains unclear. In this study, we aimed to investigate the interaction between MLH1 and the autophagy marker LC3, which facilitated nucleophagy induction, and its potential role in determining sensitivity to 5-Fluorouracil (5-FU) induced cell death. To examine the role of MLH1 in DNA-damage-induced nucleophagy in CRC cells, we utilized a panel of *MLH1* deficient and *MLH1* proficient CRC cell lines. We included a parental HCT116 cell line *(MLH1*$^{-/-}$*)* and its isogenic cell line HCT116 *MLH1*$^{+/-}$ in which a single allele of the *MLH1* gene was introduced using CRISPR-Cas9 gene editing. We observed that *MLH1* proficient cells were less sensitive to the 5-FU-induced cytotoxic effect. The 5-FU induced DNA damage led to LC3 up-regulation, which was dependent on *MLH1* overexpression. Moreover, immunofluorescence and immunoprecipitation data showed LC3 and MLH1 were colocalized in CRC cells. Consequently, MLH1 dependent 5-FU-induced DNA damage contributed to the formation of micronuclei. These micronuclei colocalize with autolysosome, indicating a cytoprotective role of MLH1 dependent nucleophagy. Interestingly, siRNA knockdown of *MLH1* in HCT116 *MLH1*$^{+/-}$ prevented LC3 upregulation and micronuclei formation. These novel data are the first to show an essential role of MLH1 in mediating the chemoresistance and survival of cancer cells by increasing the LC3 expression and inducing nucleophagy in 5-FU treated CRC cells.

Neoplasia (2022) 24, 76–85

Keywords: Colorectal cancer, Microsatellite instability, Autophagy, Nucleophagy, Chemoresistance, CRISPR-Cas9, Mismatch Repair, SIRT1, LC3, Lamin

Introduction

About 10 % of all cancer-related mortalities are attributed to colorectal carcinoma (CRC) [1]. The anticipated global burden of CRC is expected to increase by about more than 60 % by the year 2035 [2]. As a result, enormous efforts were placed on developing effective therapeutics and preventive strategies to decrease the prevalence of CRC. Interestingly, about 15 % of CRC cases develop via a pathway characterized by the DNA mismatch repair (MMR) pathway malfunctioning. CRC cases with defective MMR pathway are identified as deficient MMR (MMR-D) cancer, whereas most of the remaining CRC cases are proficient MMR (MMR-P). Most MMR-D cancers are associated with the inactivation of MutL homolog 1 (*MLH1*) or MutS homolog 2 (*MSH2*) genes. CRC patients with MMR-D are associated with high microsatellite instability (MSI-H); whereas CRCs cases with MMR-P show low microsatellite instability (MSI-L), and in most cases, are microsatellite stable (MSS). Furthermore, there are controversies about whether MSI-H is a good prognostic factor in CRC patients. Several studies

* Corresponding authors.
E-mail addresses: msaber@sharjah.ac.ae (M. Saber-Ayad), dr.jibran@live.com (J.S. Muhammad).
Received 21 September 2021; received in revised form 12 December 2021; accepted 13 December 2021

© 2021 The Authors. Published by Elsevier Inc. This is an open access article under the CC BY-NC-ND license (http://creativecommons.org/licenses/by-nc-nd/4.0/)
https://doi.org/10.1016/j.neo.2021.12.003

have shown that MMR-D CRC cases have better stage-adjusted survival than MMR-P CRC cases [3,4]. The European Society for Medical Oncology has lately excluded MSI status as a predictive marker for chemotherapy due to controversial findings [5]. Nevertheless, it is widely accepted that MSI-H cancer patients with better survival show less metastasis, and whether MSI patients benefit more from 5-Fluorouracil (5-FU) therapy than the MSS CRC patients is controversial.

MLH1 is a crucial component of the MMR pathway [6], and is implicated in other key cellular processes such as cell cycle regulation and apoptosis [7]. Another process implicated in CRC tumorigenesis and therapeutic resistance is autophagy [8]. Autophagy may exert protective functions during advanced stages of cancer by supplying cancer cells with extra building blocks and energy sources to meet their demands. Recently, autophagy has been observed to protect cancer cells from chemotherapy-mediated apoptosis by inducing senescence [9]. Cellular senescence is a phenomenon of attaining stable cell cycle arrest, particularly in response to DNA damage. Thus, autophagy is considered one of the integral steps cancer cells use in the stress adaption process for aggressiveness, metastasis, and senescence. Only a few studies have linked chemotherapy-induced autophagy with MMR pathway genes, but a plethora of questions remain unanswered.

Given that autophagy is induced in response to DNA damage and that MLH1 status affects CRC aggressiveness, we hypothesized that MLH1 could influence the anticancer drug response by mediating DNA damage-induced autophagy of the nuclear material. Using a panel of *MLH1* proficient and *MLH1* deficient CRC cell lines, as well as an isogenically matched *MLH1* gene CRISPR-Cas9 knock-in CRC cell line, we showed that MLH1 mediates the resistance to chemotherapy-induced DNA damage by favoring nucleophagy in CRC cells. For the first time, we showed an essential role of MLH1 in mediating the survival of CRC cells by increasing the LC3 expression, inducing nucleophagy upon 5-FU treatment.

Methods

Cell lines

A panel of four CRC cell lines was utilized in this study. SW480 (RRID: CVCL_0546) and RKO (RRID: CVCL_0504) cell lines were obtained from American Type Culture Collection (ATCC, Manassas, VA, USA). Also, a pair of isogenic cell lines, HCT 116 parental (RRID: CVCL_0291) and HCT 116 MLH1+/- CRISPR-Cas9 knock-in (RRID: CVCL_HD84; knock-in by homologous recombination of the wild-type *MLH1* in 1 of the 2 alleles), were obtained from Horizon Discovery, gene editing company (Cat. no# HD104-006, Waterbeach, UK). These cell lines were chosen to match the CMS group of HCT 116 (all four cell lines used are CMS4; both HCT 116 and RKO are MSI-H, SW480 is MSI-L). These CRC cells were cultured at 37 °C in humidified 95% air, 5% CO_2 and regularly evaluated for mycoplasma contamination. All these cell lines were maintained in RPMI culture media supplemented with 10 % FBS and 1 % penicillin and streptomycin. Cells were seeded at 1×10^6 cells/mL in a 100 mm dish. When reaching about 70 % confluence, they were treated with 5-Fluorouracil (5-FU), Doxorubicin (DOX) and Irinotecan purchased from Sigma (Sigma Aldrich, MO, USA) at increasing concentrations diluted in DMSO. Control cells were left untreated and are referred to as untreated cancer cells. Results were normalized to the effects of cell culture media on these control cells.

Cell viability assay

CRC cell lines were treated with different concentrations of 5-FU, DOX, Irinotecan or a DMSO vehicle control in triplicates. Briefly, 5000 cells/well were seeded in 96-well plates and treated with different concentrations of 5-FU, DOX and Irinotecan. After 24 h or 48 h, viability assays were performed using an MTT assay (Sigma Aldrich) and a Biotek plate reader. After subtracting the values of media blank, viability was calculated following normalization to the control. Values represent an average of three independent experiments.

Flow cytometric analysis for apoptosis

To assess apoptosis, an Annexin V-FITC/PI apoptosis kit (Annexin v-FITC Early Detection Kit #6592, Thermo Fisher Sci., MA, USA) was used according to the manufacturer's instructions. Briefly, cells were seeded at a density of 1×10^6 cells per 10 mm culture dish. After attachment overnight, cells were washed twice, collected, suspended with PBS, and cultured in a medium with 5 µM and 10 µM for 24 h or 48 h. All cells were collected and suspended in an ice-cold 1x binding buffer. Approximately 1×10^5 cells were then stained with 1 µL of Annexin V-FITC and 12.5 µL of PI for 15 min and analyzed using a Flow cytometer (BD FACS Aria III; Becton Dickinson, NJ, USA).

Western blot analysis

Cells were lysed in RIPA buffer and cleared by centrifugation (14,000 RPM for 15 min at 4°C). Protein concentration was determined using the bicinchoninic acid assay (BCA) method. Cell lysates containing 20 µg protein were separated by SDS-PAGE gel electrophoresis and transferred onto a Polyvinylidene difluoride membrane (BioRad). The membranes were blocked with 5 % skimmed milk powder (Sigma Aldrich) for 1 h at room temperature, washed with TBST, and reacted with primary antibody anti-LC3(A/B)-I/II, anti-Beclin, anti-ATG3, anti-ATG5, anti-ATG16, anti-H2AX, anti-SIRT1, anti-MLH1, anti-Lamin A/C, anti-PARP, or anti-GAPDH (all antibodies were from Cell Signaling Technology, MA, USA) at 1:1000 dilution overnight at 4°C. The specific HRP-labeled secondary antibodies (Cell Signaling Technology) were then reacted at 1:2000 dilutions for 1 h at room temperature. Chemiluminescence was detected using Enhanced Chemiluminescence western blotting detection reagent (BioRad, CA, USA). GAPDH or PARP was used as a loading control.

Nuclear staining and immunofluorescence microscopy

Cells were seeded onto glass coverslips and cultured in 6 well plates at 37°C. After incubation, cells were fixed with 4 % formaldehyde for 30 min and permeabilized with 0.1% Triton X-100 in PBS for 10 min. The cells were stained using 4′, 6-Diamidino-2-phenylindole dihydrochloride (Sigma Aldrich). Images were captured using an IX73 inverted microscope system.

Autophagy analysis

To assess cellular autophagy, an autophagosome formation detection kit (Sigma Aldrich, MAK138) was used according to the manufacturer's instructions. Briefly, cells were cultured in appropriate conditions for 18 h and then treated with or without 5-FU for 24 h. Untreated cells were used as controls. Chloroquine (CQ; 50 µM), an autophagy inhibitor-treated cells were used as a negative control. All experiments were conducted in triplicate and repeated 3 times. Western blotting was used to assess the basal level of autophagy by measuring autophagy marker LC3 I/II protein expression. Confocal microscopy was used to determine the autophagy flux by measuring colocalization of autophagosomes with lysosomes by incubating the cells with 60 nM of LysoTracker (Life Technologies) for 1hr at room temperature.

Nuclear and cytoplasmic protein extraction from cultured cell lines

The separation of proteins from cell cultures into nuclear and cytoplasmic fractions was carried out using a subcellular protein fractionation kit for

cultured cells (Thermo Scientific) as per the manufacturer's instructions. Extracted nuclear and cytoplasmic protein fractions were frozen (-80 °C).

EGFP-LC3 transfection

Isogenically matched *MLH1* proficient HCT116 MLH1$^{+/-}$ cells were transfected with LC3-GFP (Premo™ Autophagy Sensor LC3-GFP BacMam 2.0) according to the manufacturer's instructions. The cells were transiently transfected for 24 h and then treated with the indicated reagents. Laser scanning confocal microscopy was used to image the cells (GFP scanning: λex = 530 nm and λem = 500 nm).

RNA interference

Isogenically matched *MLH1* proficient HCT116 MLH1$^{+/-}$ cells were transfected with Silencer® small interfering RNA (siRNA) for knockdown of *MLH1* (siMLH1 '119549' Catalog # AM51331, purchased from Thermo Fisher Sci.). These Silencer siRNAs are pre-designed and pre-validated for maximum potency and specificity. Silencer Select Negative Control siRNA (Thermo Fisher Sci., catalog # 4390843) was used as a negative control. For high throughput transfection, the reverse transfection method was performed using Lipofectamine 2000 and Opti-MEM Reduced Serum Medium (Life Technologies) as described previously [10].

Immunoprecipitation assay

The immunoprecipitation assay was performed according to the manufacturer's instructions using an immunoprecipitation kit (ab206996, Abcam, Cambridge, UK). At least two independent experiments were performed to assess the physical interaction of MLH1 and LC3. The cells were lysed in a non-denaturing lysis buffer. Then the protein lysate was incubated with MLH1 antibody (4C9C7-Cell Signaling Technology) overnight at 4°C. The beads were washed three times with wash buffer and blocked with BSA for 1 h. The BSA was then removed and three washings were performed. Beads were added to the antibody-protein lysate mixture and incubated at 4°C for 1 h. Beads were again washed three times with wash buffer, and then the complex was eluted in 2X lamellae buffer after boiling for 5 min. The eluent was stored at -80°C until the SDS-PAGE and immunoblotting were performed.

Statistical analysis

All the graphs and statistical analyses were prepared using GraphPad Prism software version 8.0 (San Diego, CA, USA). Results are expressed as mean ± SD. The comparisons were performed using one-way or two-way analysis of variance (ANOVA). $^{*}p < 0.05$ was regarded as significant.

Results

MLH1 proficient cells are resistant to DNA damage as compared to MLH1 deficient cells

There is much controversy in predicting the association of MSI status with the chemotherapeutic response [5]. We conducted *in silico* analysis using the Genomics of Drug Sensitivity in Cancer (GDSC; www.cancerRxgene.org) to investigate this issue, searching for the half-maximal inhibitory concentration (IC50) values for the *MLH1* deficient and proficient CRC cell lines in response to 5-FU treatment. Based on the work by Kaja et al., characterization of CRC cell lines for presence and absence of mutations in *MLH1* gene by targeted sequencing, we selected ten CRC cell lines for *in silico* analysis [11]. Figure 1A shows that all five of the *MLH1* proficient CRC cell lines (SW1116, SW620, SW948, LS-1034, and COLO-320) showed higher 5-FU IC50 values than the four of the five *MLH1* deficient CRC cell lines (HCT116, HCT-15, RKO, and KM12), only except for SW48 cell line. Next, we experimentally validated MLH1 status in a set of four CRC cell lines. Here, isogenic CRISPR-Cas9 knock-in *MLH1* proficient HCT116 MLH1$^{+/-}$ cells and HCT116 parental (MLH1$^{-/-}$) cells were used. Additional cell lines used to support the findings included RKO (*MLH1*-deficient) and SW480 (*MLH1*-proficient). The MLH1 protein expression in these cell lines was confirmed by western blotting (Figure 1B).

We evaluated the effects of 5-FU treatment on HCT116 parental and HCT116 MLH1$^{+/-}$ cell viability using a standard MTT assay. 5-FU treatment profoundly affected the viability of *MLH1* deficient cells in a time and dose-dependent manner. In contrast, 5-FU treatment did not significantly affect *MLH1* proficient cells compared to *MLH1* deficient cells (Figure 2A). We further assessed the viability of *MLH1* proficient HCT116 MLH1$^{+/-}$ and *MLH1* deficient HCT116 parental cells using two additional DNA-damaging drugs, Doxorubicin and Irinotecan. MTT analysis revealed that Doxorubicin and Irinotecan significantly affected the cell viability of *MLH1* deficient HCT116 parental cells compared to *MLH1* proficient HCT116 MLH1$^{+/-}$ cells in a dose- and time-dependent manner (Supplementary Figure S1), confirming our previous results. Next, we confirmed apoptosis induction in a panel of *MLH1* proficient and *MLH1* deficient cell lines using the Annexin-PI staining. Our results showed that 5-FU treatment remarkably increased the number of apoptotic cells in *MLH1* deficient cells compared to the *MLH1* proficient cells in a time and dose-dependent manner ($P < 0.05$; Figure 2B and C). These results suggested that the *MLH1* gene could be responsible for CRC cell's hyposensitivity towards the DNA damage induced by 5-FU treatment.

MLH1 influences 5FU-induced autophagy in CRC cell lines

It is well known that autophagy is one of the cellular protein degradation pathways which may lead to chemoresistance [12]. To determine the effect of the *MLH1* gene on the 5-FU-induced autophagy, we investigated the level of LC3-I/II and the formation of autophagosomes in *MLH1* proficient HCT116 MLH1$^{+/-}$ cells and *MLH1* deficient HCT116 parental CRC cells. Western blot analysis revealed that MLH1 increased the expression of the autophagy markers LC3-II, Beclin, ATG16, ATG5 and ATG3 in 5-FU treated *MLH1* proficient HCT116 MLH1$^{+/-}$ cells compared to *MLH1* deficient HCT116 parental cells (Figure 3A and 3B). We also investigated the LC3-I/II levels in SW480 and RKO cell lines. Western blotting revealed that *MLH1*-proficient SW480 cells expressed more LC3-II than *MLH1* deficient RKO cells after treatment with 5-FU (Figure 3C). The increase in LC3-II levels may be due to more autophagy or inhibition of autophagy at later stages. To ensure that the increase in LC3-II levels in *MLH1* proficient cells HCT116 MLH1$^{+/-}$ may not be due to late-phase autophagy inhibition, we measured LC3-II in *MLH1* proficient HCT116 MLH1$^{+/-}$ cells treated with lysosomal inhibitor chloroquine. The further increase in LC3-II levels in chloroquine treated cells compared to LC3-II levels in 5-FU treated cells suggested the increase in LC3-II levels in *MLH1* proficient cells is plausibly due to increased autophagy (Figure 3D). Furthermore, autophagosome detection assay showed that *MLH1*-proficient HCT116 MLH1$^{+/-}$ cells produced substantially more autophagosomes than the *MLH1*-deficient HCT116 parental cells after treatment with 5-FU (Figure 3E), indicating that the increased rate of DNA damage-induced autophagy depends on the *MLH1* gene.

Nuclear-cytoplasmic ratio of MLH1, LC3, and SIRT1 changed after 5-FU induced DNA damage

A recent study suggested that DNA damage leads to the induction of nucleophagy, a form of selective autophagy [13]; hence one would expect

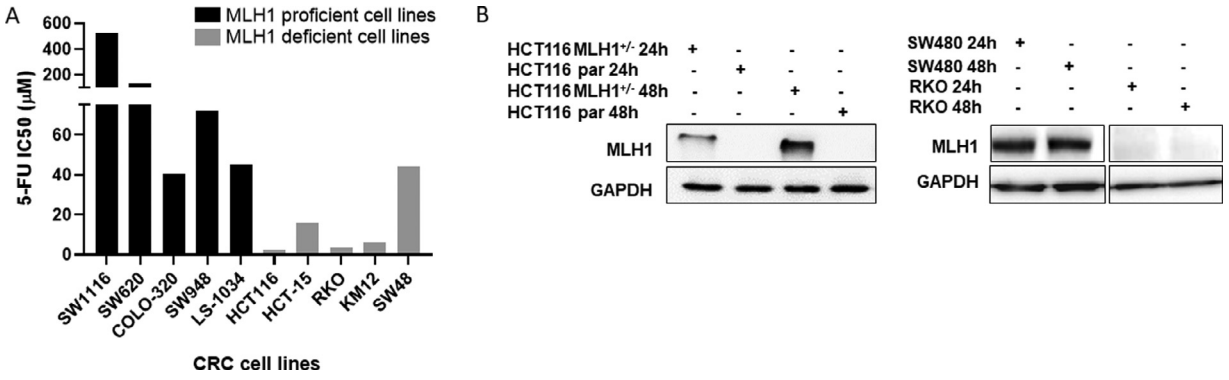

Figure 1. *In silico* analysis of ten CRC cell lines revealed *MLH1* proficient colorectal cancers correlates to higher IC50 values of DNA damage-inducing drug 5-FU (A). Confirmation of MLH1 expression in a panel of four CRC cancer cell lines at 24 h and 48 h (B).

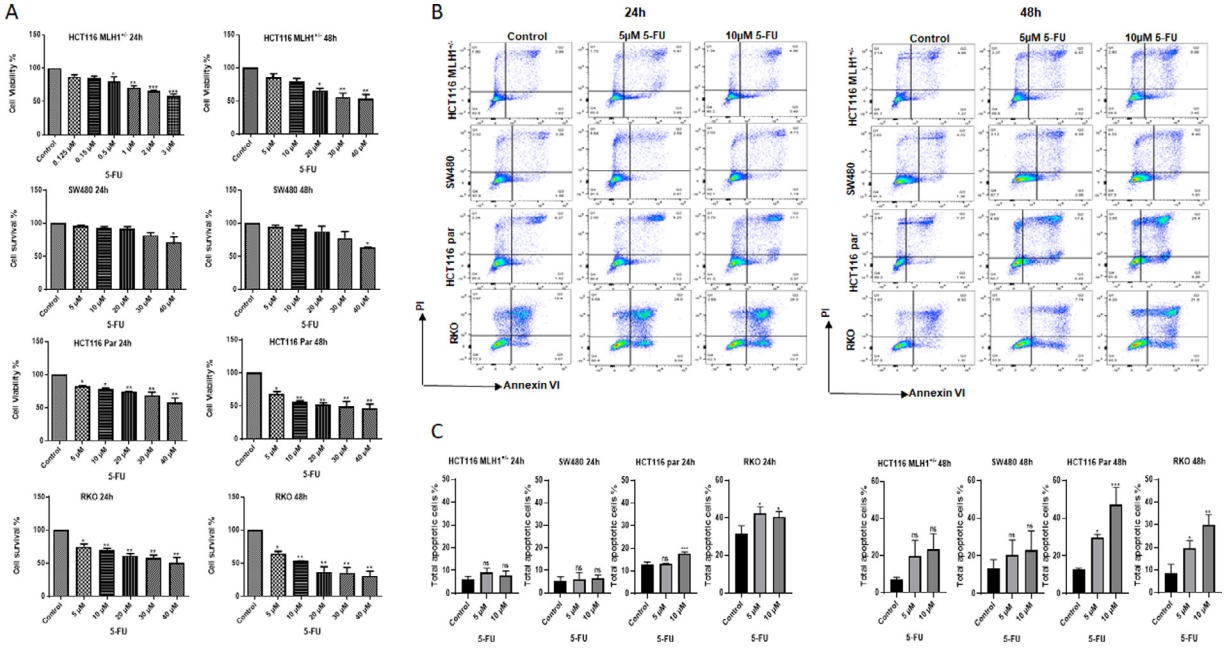

Figure 2. MLH1 increases hyposensitivity to 5-FU in colorectal cancer. The viability of *MLH1* proficient cells HCT116 MLH1$^{+/-}$, SW480 and *MLH1* deficient cells HCT116 par (parental), RKO was assessed by MTT assay after treatment with 5-FU for 24 h and 48 h (A). Total apoptosis in a panel of CRC cell lines was measured by Annexin PI-FITC staining after treatment with 5-FU for 24 h and 48 h (B). Graphs represent quantification of total apoptosis after treatment with 5-FU for 24 h and 48 h in a panel of CRC cell lines (C). One-way ANOVA ****$p \leq 0.0001$, ***$p \leq 0.001$ **$p \leq 0.01$, *$p < 0.05$.

an increase in phosphorylated H2AX as a DNA damage marker when nucleophagy is induced. H2AX plays a vital role in DNA damage repair, and, as previously, it was demonstrated that H2AX degradation occurring via proteasomal pathway caused cells to become more sensitive to chemotherapy due to inefficient DNA repair [14,15]. Therefore, to confirm DNA damage in *MLH1* proficient HCT116 MLH1$^{+/-}$ and *MLH1* deficient HCT116 parental cells, we assessed the level of 5-FU-induced DNA damage by measuring phosphorylation of H2AX. Our results show a considerable increase in the expression of the phosphorylated H2AX in a dose-dependent manner in *MLH1* proficient cells compared to the HCT116 deficient cells (Figure 4A). Our immunofluorescence results also demonstrated a substantial increase in the phosphorylated H2AX in *MLH1* proficient HCT116 MLH1$^{+/-}$ cells in a dose-dependent manner (Figure 4 A, B), indicating that higher phosphorylation of H2AX might enhance the capability of cells to survive via nucleophagy. The Sirtuin family of proteins is comprised of nicotinamide adenine dinucleotide (NAD+)–dependent deacetylases that regulate transcription within the cells. Among the sirtuin family, SIRT-1 is the most extensively studied and expressed protein [16]. Recently, SIRT-1 has been shown to be crucial for the deacetylation of LC3 and subsequent transport to the cytoplasm to initiate autophagosome formation. [17] Next, we investigated whether the *MLH1* gene could influence the autophagy-related protein LC3 and SIRT1 nucleocytoplasmic dynamics. We evaluated autophagy activity by examining LC3-II in both cytoplasmic and nuclear extracts using *MLH1*-deficient CRC cell lines, HCT116 parental cells, and the isogenically matched *MLH1*-proficient, HCT116 MLH1$^{+/-}$ cells. The absence of cross-contamination between the fractions was confirmed using GAPDH and PARP antibodies. Western blot results showed that 5-FU related DNA damage induced the shuttling of LC3 and MLH1 proteins to the cytoplasm in a dose-dependent manner. The data also show that MLH1 and LC3 were mainly localized in the nucleus before 5-FU induced DNA damage. The DNA damage-induced a gradual increase in MLH1 and LC3 protein ratio in the cytoplasm, while nuclear MLH1 and LC3-II were decreased. Furthermore, SIRT1 was examined in subcellular fractions. In contrast to MLH1 and LC3, SIRT1 was increased in both the nuclear and

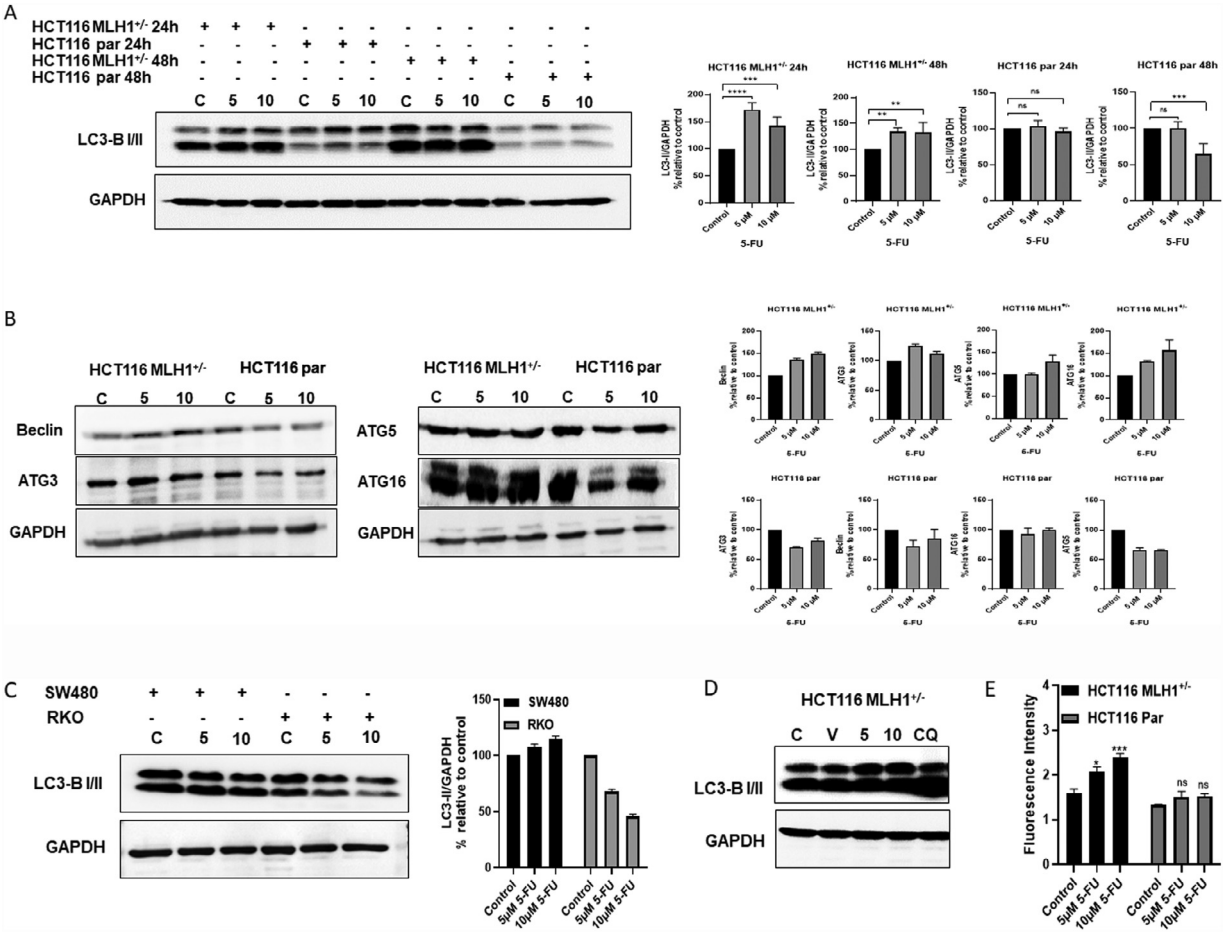

Figure 3. MLH1 increases 5-FU induced Autophagy Flux. Autophagy flux was assessed by measuring LC3-II expression by western blotting in HCT116 MLH1$^{+/-}$ cells and HCT116 par (parental) cells after treatment with 5 μM and 10 μM of 5-FU for 24 h and 48 h. Graphs represent the quantification of LC3-II expression in HCT116 MLH1$^{+/-}$ cells and HCT116 par (parental) cells in a dose and time-dependent manner. One way ANOVA $^{****}p \leq 0.0001$, $^{***}p \leq 0.001$ $^{**}p \leq 0.01$ (A). Expression of autophagy-related proteins Beclin, ATG16, ATG5 and ATG3 in HCT116 MLH1$^{+/-}$ cells and in HCT 116 par (parental) cells after treatment with 5 μM and 10 μM of 5-FU (B). Expression of LC3-II was measured in the *MLH1* proficient SW480 cells and *MLH1* deficient RKO cells after treatment with 5 μM and 10 μM of 5-FU (C). LC3-II expression was measured in *MLH1* proficient HCT116 MLH1$^{+/-}$ cells after treatment with 5-FU and Chloroquine 50 μM (D). Autophagosome formation was detected by fluorescent staining of autophagic vacuoles in HCT116 MLH1$^{+/-}$ cells compared to HCT116 par (parental) cells after treatment with 5 μM and 10 μM of 5-FU. Two-way ANOVA $^{***}p \leq 0.001$, $^{*}p < 0.05$ (E).

cytoplasmic compartments after 5-FU induced DNA damage. On the other hand, *MLH1* deficient HCT116 parental cells failed to show an increase or shuttling of LC3-II within the cellular compartments (Figure 4 C, D, and E). These results suggest that MLH1 and SIRT1 may directly interact to induce nucleophagy.

MLH1 is required for DNA damage-induced nucleophagy

Nuclear protrusions have been associated with the autophagy of nuclear material [18]. Consequently, we visualized nuclear morphology using confocal microscopy following induction of DNA damage by performing DAPI staining. As shown in Figure 5A, *MLH1* proficient cells HCT116 MLH1$^{+/-}$ showed a significantly increased change in nuclear morphology as indicated by increased nuclear protrusions (micronuclei), and DAPI positive particles at 24 h and 48 h in comparison to the *MLH1* deficient cells, the HCT116 parental cells in a dose-dependent manner ($p<0.05$) (Figure 5B). These results suggested that MLH1 may favor DNA damage to induce nucleophagy. A nuclear repair mechanism known as nucleophagy has been shown to degrade DNA damaged areas of a nuclear component, maintaining its integrity and function [19]. To understand the functional role of MLH1 in regulation of 5-FU induced LC3 upregulation, we knocked down the *MLH1* gene in *MLH1*-proficient HCT116 cells. Our results showed that knockdown of *MLH1* in proficient cells inhibited 5-FU induced LC3 upregulation in western blot as well as in immunofluorescence (Figure 5C and 5D right corner panel). To determine whether MLH1 is involved in DNA damage-induced autophagy, *MLH1* proficient HCT116 MLH1$^{+/-}$ and *MLH1* deficient HCT116 parental cells were treated with various doses of 5-FU and incubated with anti-LC3 antibody (autophagosome marker) and DAPI (DNA marker). The presence of autophagosome accumulation was detected using a confocal laser-scanning microscope. More colocalization of autophagosomes (green) and micronuclei DNA (blue) was observed in the *MLH1* proficient HCT116 MLH1$^{+/-}$ cells treated with 5-FU compared to *MLH1* deficient HCT116 parental cells ($p<0.05$). On the other hand, in *MLH1* deficient HCT116 parental cells, DNA damage did not show the formation of autophagosomes and its fusion with lysosomes around the perinuclear sites. Additionally, immunofluorescence analysis demonstrated that knockdown of *MLH1* in HCT116 MLH1$^{+/-}$ cells decreased the formation of micronuclei and

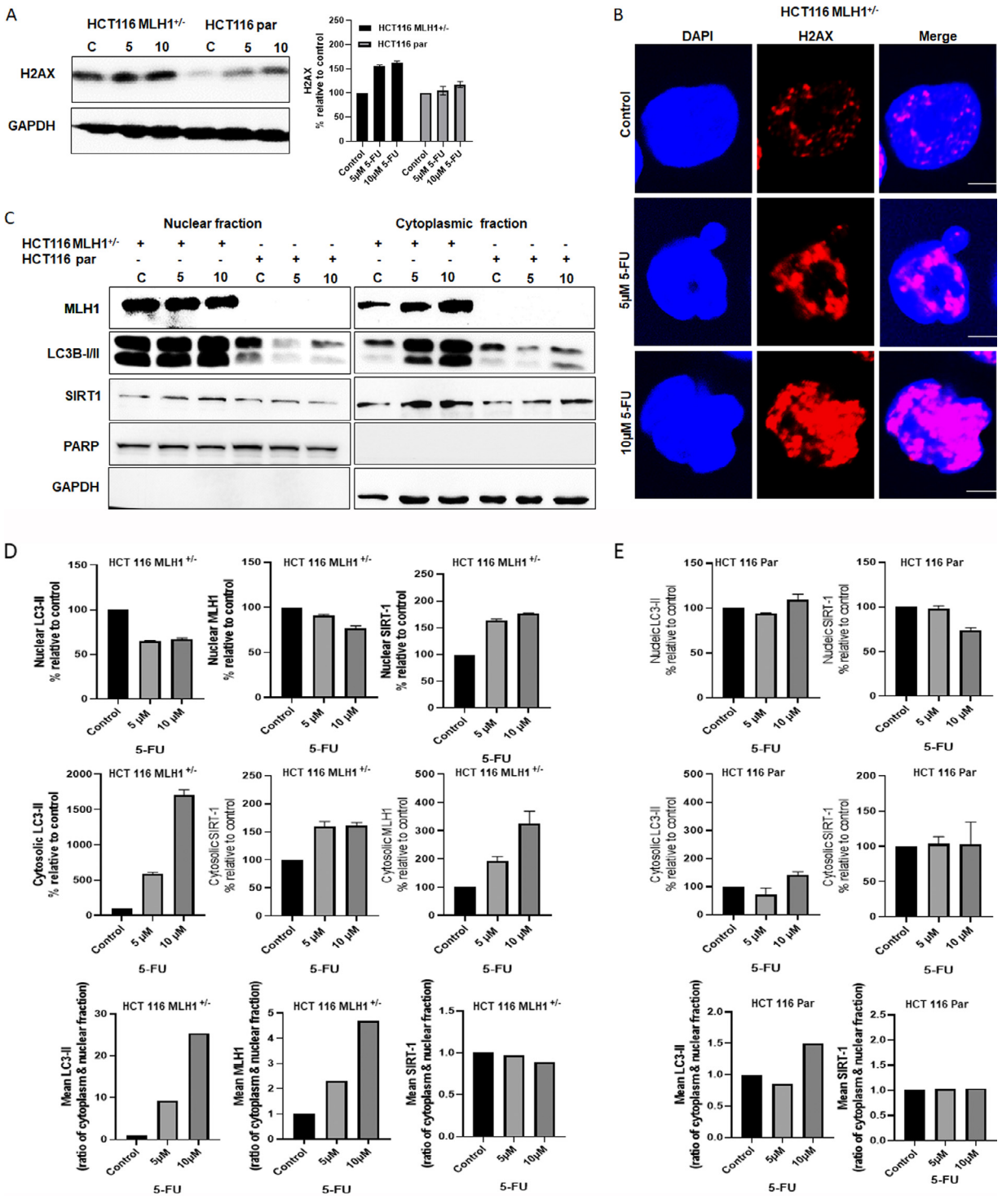

Figure 4. Nucleocytoplasmic ratio of MLH1, LC3 and SIRT1 changed after 5-FU induced DNA Damage. H2AX expression in HCT116 MLH1+/- cells and HCT116 par (parental) cells after treatment with 5μM and 10μM of 5-FU (A). Representative immunofluorescence images of HCT116 MLH1+/- cells were incubated with H2AX antibody and DAPI (DNA) (B). Subcellular protein expression of MLH1, LC3-I/II and SIRT 1 in HCT116 MLH1+/- cells and HCT116 par (parental) cells treated with 5 μM and 10 μM of 5-FU for 48h (C). Graph showing quantification of LC3-II, MLH1, and SIRT1 overall expression and their ratio in subcellular compartments of HCT116 MLH1$^{+/-}$ cells and HCT116 par (parental) cells after treatment with 5-FU (D and E). Scale bar 20μm.

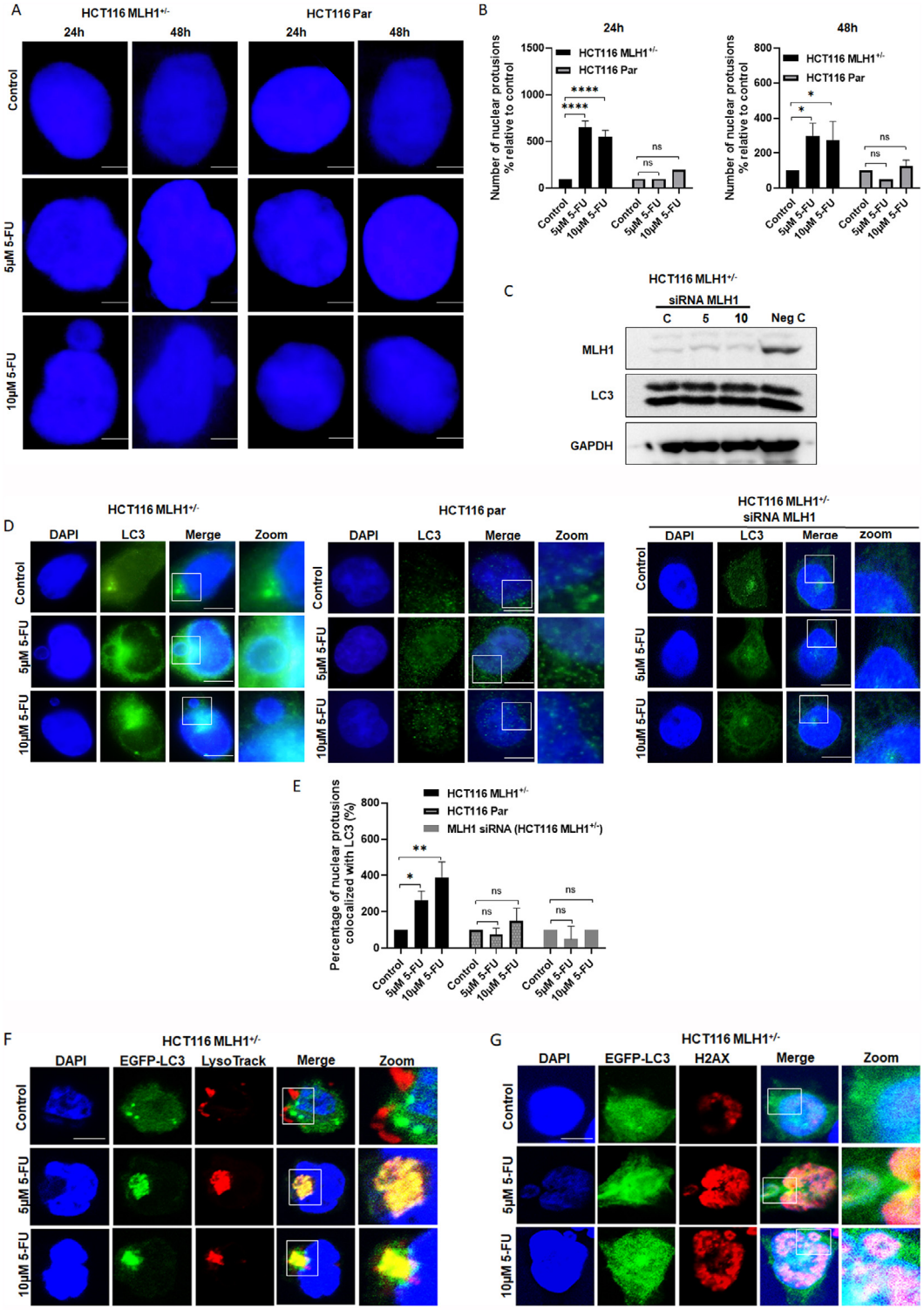

Figure 5. MLH1 is required for DNA damage-induced nucleophagy. Representative immunofluorescence images of micronuclei formation after 5-FU treatment in HCT116 MLH1$^{+/-}$ cells compared to HCT116 par (parental) cells scale bar 10μM (A). Graph showing quantification of micronuclei in HCT116 MLH1$^{+/-}$ cells treated with 5-FU at 24 and 48 h,. One-way ANOVA ****$p \leq 0.0001$, *$p < 0.05$ (B). *MLH1* proficient cells transfected with siRNA MLH1 were treated with 5 μM and 10 μM of 5-FU. Expression of LC3 and MLH1 was observed by western blotting (C). Representative immunofluorescence images of autophagosome (LC3 puncta) and leaked DNA (DAPI) colocalization in *MLH1* proficient HCT116 MLH1$^{+/-}$ cells in comparison to *MLH1* deficient HCT 116 par (parental) cells and *MLH1* proficient cells treated with siRNA MLH1 (D). Quantification of micronuclei colocalized with LC3 in *MLH1* proficient HCT116 MLH1$^{+/-}$ cells compared to *MLH1* deficient HCT 116 par (parental) cells after treatment with 5-FU, Two-way ANOVA *$p<0.05$ (E). The autolysosome's representative immunofluorescence images of autolysosome colocalized with leaked DNA in *MLH1* proficient HCT116 MLH1$^{+/-}$ cells (F). Representative immunofluorescence images of autophagosome (LC3) colocalized with DNA damage marker H2AX and leaked DNA (DAPI) (G). Scale bar 20μm.

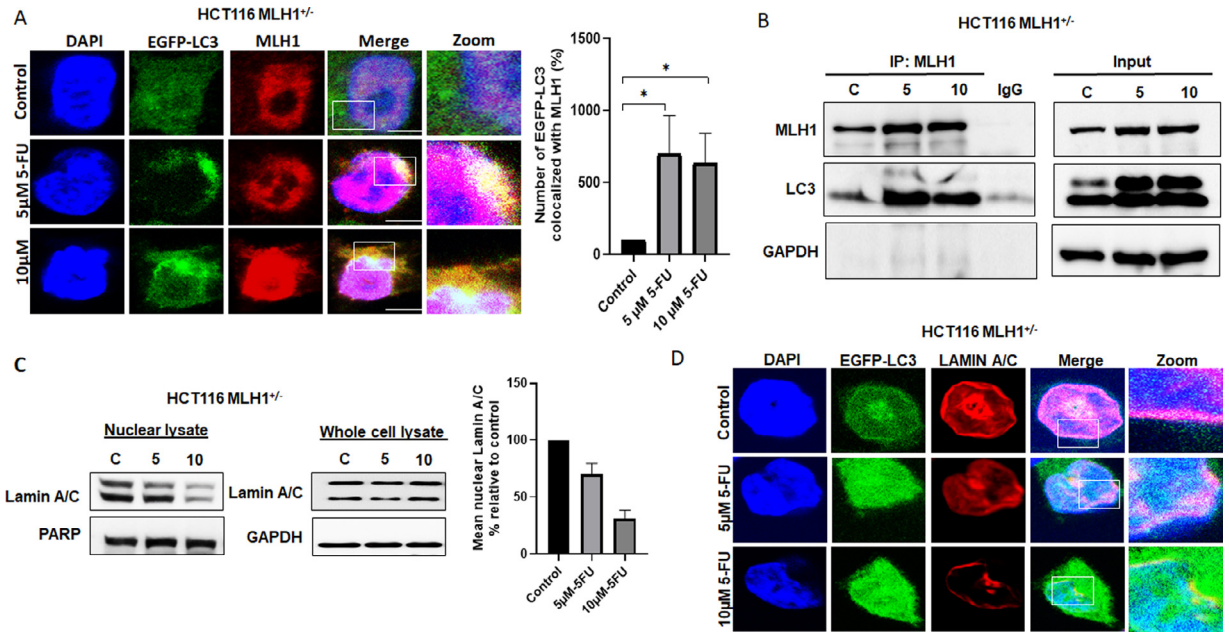

Figure 6. MLH1 and LC3 interplay influences nucleophagy substrate protein Lamin A/C. MLH1 colocalizes with LC3 and micronuclei (DAPI) in *MLH1* proficient HCT116 MLH1+/-cells treated with 5-FU, Graph showing quantification MLH1 colocalized with LC3 and DNA, One-way ANOVA *p<0.05 (A). Cell lysate was co-immunoprecipitated with anti-MLH1 antibody and immunoblotted with anti-LC3 (B). Expression of Lamin A/C in nuclear fraction and whole cell lysate of *MLH1* proficient HCT116 MLH1$^{+/-}$cells after treatment with 5-FU. Graph showing quantification of nuclear Lamin A/C in HCT116 MLH1$^{+/-}$ cells after treatment with 5-FU. (C) Representative immunofluorescence images of autolysosome colocalized with Lamin A/C and DNA (DAPI) in *MLH1* proficient HCT116 MLH1$^{+/-}$ cells (D). Scale bar 20μm.

autophagosomes marked by LC3 (Figure 5C, D, E). These findings further confirm the important functional role of MLH1 in DNA damage induced nucleophagy.

As autophagy progresses, autophagosomes begin fusion with lysosomes, leading to autolysosome formation. To visualize autolysosome colocalization with micronuclei, we transfected cells with EGFP-LC3 (green) and incubated them with LysoTracker (red). We observed that 5-FU treatment induced LC3-GFP to be primarily present at the perinuclear site of *MLH1* proficient cells in a dose or time-dependent manner. At the same time, lysosomes marked by LysoTracker red, migrated towards the perinuclear region, where most began to fuse with autophagosomes to form autolysosomes. Interestingly, a strong DAPI signal could be found in these particles, suggesting DNA material was encapsulated within the autophagosomes (Figure 5F). To test whether micronuclei fused with autolysosomes contained damaged DNA, we transfected *MLH1* proficient HCT116 MLH1$^{+/-}$ cells with EGFP-LC3 and treated them with 5-FU following incubation with an anti-H2AX antibody. The presence of colocalized H2AX-positive micronuclei with autophagosomes was detected with confocal laser scanning microscopes (Figure 5G).

MLH1 and LC3 interplay influences nucleophagy substrate protein Lamin A/C

Next, we sought to determine whether DNA damage may lead to MLH1 and LC3 interplay. To investigate the molecular interaction between MLH1 and LC3, we examined MLH1 and LC3 colocalization with the micronuclei following the 5-FU induced DNA damage. Briefly, EGFP-LC3 was transfected in *MLH1* proficient HCT116 MLH1$^{+/-}$ cells. Following the 5-FU induced DNA damage, the cells were stained with an anti-MLH1 antibody. Figure 6A shows DNA damage-induced the translocation of MLH1 to the cytoplasm in a dose-dependent manner. Notably, MLH1 and LC3 partially colocalized near the perinuclear site. As this immunofluorescence and previous western blotting results indicated that MLH1 influences LC3 after 5-FU treatment, we further confirmed MLH1 and LC3 interaction by using immunoprecipitation assays. Interestingly we found MLH1 pull down caused LC3 to be co-immunoprecipitated. As shown in the Figure 6B co-immunoprecipitation assay provided evidence for molecular interaction between MLH1 and LC3, this interaction was further increased upon 5-FU treatment.

Nuclear lamina plays a crucial role in maintaining the structural integrity of the nuclear envelope [20]. A recent study demonstrated that Lamin A/C is a nucleophagy substrate in response to DNA damage. In addition, nucleophagy was responsible for the degradation of Lamin A/C and the release of nuclear DNA [13]. To determine whether DNA damage altered the levels of Lamins, we tested the changes of Lamin A/C in nuclear extract, and whole cell lysate of 5-FU treated *MLH1* proficient HCT116 MLH1$^{+/-}$ cells.

In response to 5-FU treatment, we observed a dose-dependent decrease of Lamin A/C content in *MLH1* proficient HCT116 MLH1$^{+/-}$ cell in the nuclear fraction. However, no alterations in Lamin A/C levels were found in whole-cell extracts, suggesting nucleophagy mediated Lamin A/C degradation (Figure 6C). Next, we studied whether autophagosomes and Lamin A/C colocalize with DNA after 5-FU treatment. We examined colocalization of LC3, Lamin A/C, and DNA (DAPI staining) in *MLH1* proficient HCT116 MLH1$^{+/-}$ cells using confocal microscopy. Figure 6D shows that Lamin A/C colocalizes with LC3 and DNA after 5-FU treatment suggesting activation of nucleophagy. Taken together, these findings indicate that DNA damage induces LC3-MLH1 interaction and leads to nucleophagy induction. The activated LC3-MLH1-LaminA/C complex results in the degradation of damaged nuclear components for energy, maintenance of nuclear homeostasis, and survival.

Discussion

In CRC, deficiency in the DNA MMR pathway proteins, such as MLH1, MSH2, and MSH6, leads to microsatellite errors resulting in hypermutated MSI tumors, which differ from MSS cancers based on their mutation

profiles. Much controversy surrounds the association of MSI with the 5-FU chemotherapy response in patients with CRC. Several studies reported that patients with MMR-D CRC have better survival rates than those with MMR-P [3,4]. Since MSI can result from mutations in one or more of the MMR genes, this study aims to determine the role of MLH1 in anticancer drug resistance and CRC tumorigenesis.

In this study, we demonstrated that MLH1 promotes cell homeostasis by upregulating autophagy-related proteins LC3 and stress marker SIRT1 in response to 5FU-induced cytotoxic effects through its interaction with LC3 and subsequent degradation of leaked nuclear content (see Graphical Abstract). Autophagy is a critical catabolic pathway for degrading cellular material [21]. The degradation of nuclear components through the autophagic pathway is called nucleophagy [19]. Recent studies suggested that LC3, stored in the nucleus, plays an essential role in the degradation of damaged nuclear material [22]. However, the exact mechanism remains to be determined. Considered a tumor suppressor, the *MLH1* gene has been related to CRC aggressiveness, indicating its contextual role [23,24]. Using an isogenically matched *MLH1* gene CRISPR-Cas9 knock-in cell line, we showed a novel role of the MLH1 in causing DNA damage-dependent induction of autophagy in nuclear components. Our western blotting analysis confirmed that DNA damage, measured by H2AX, increases the level of LC3 in *MLH1* proficient cells. Furthermore, confocal microscopy demonstrated that LC3 and MLH1 colocalized preceding the DNA damage.

The role of DNA repair protein MLH1 is diverse. Apart from its central role in mismatch repair, it is involved in multiple cellular processes like apoptosis and cell cycle progression [7]. In the present study, we focused on MLH1 and nuclear autophagy and found a clear correlation between MLH1 and the autophagy marker LC3 protein in the nucleus of CRC cells. We observed that MLH1 leads to hyposensitivity to DNA damage-inducing agents by regulating LC3 expression. We observed that MLH1 upregulates LC3, Beclin, ATG 16, ATG5 and ATG3 and thus reduces the DNA damage effect expected by chemotherapeutic agents. The autophagy protein LC3 plays an essential role in the mechanism of autophagy. The LC3 protein is the key marker of the autophagy pathway, leading to both cargo selection and autophagosome formation in the cytoplasm [25]. In this study, we demonstrated that LC3 localization was correlated with the expression of MLH1 in the cells and that LC3 -II levels were dependent on MLH1 expression. For further confirmation of functional role of MLH1 in nucelophagy was achieved by knockdown of *MLH1* gene, which inhibited DNA damage induced increase. LC3 levels and attenuated the formation of micronuclei, autophagosomes, and their colocalization. Finally, by using immunoprecipitation analysis, for the first time, we found that DNA damage promoted physical interaction of MLH1 with LC3. Altogether our data demonstrated DNA damage may promote interaction of MLH1 and LC3 resulting in induction nucleophagy which may result in recycling of damaged DNA.

Recent studies have shown that SIRT1 is necessary for the deacetylation of LC3 and autophagy activation [17]. Previously, SIRT1 was found to induce autophagy and protected cardiomyocytes from undergoing apoptosis [26]. We further investigated the mechanistic link between MLH1 and autophagy by determining the SIRT1 protein levels and demonstrated that MLH1 dependent SIRT1 upregulation followed the DNA damage induction. Previous studies also showed that nuclear LC3 plays a significant function in degrading damaged nuclei and nuclear components [22]. Our data demonstrated that MLH1 contributed to the formation of DNA damage-induced micronuclei that were surrounded by abundant autophagosomes and autolysosomes.

The evidence for the involvement of nuclear Lamin proteins in nucleophagy has been increasing. A previous study indicated that autophagy proteins interact directly with the nuclear Lamin protein, Lamin B1 [27]. Another study reported that mutations in Lamin A/C increase nuclear DNA leakage in response to DNA damage, suggesting that Lamin defects might trigger autophagy to destroy damaged nuclear DNA [13]. In this study, we demonstrated that DNA damage promotes interaction between Lamin A/C and LC3 molecules. This interaction reduces Lamin A/C levels in the nucleus of cells proficient in MLH1 expression. Furthermore, using the isogenic *MLH1* CRISPR-Cas9 knock-in HCT116 cell line, we showed that the MLH1-dependent nucleophagy induction might contribute to the acquisition of DNA damage-inducing therapy-resistant phenotype. We further showed that the autophagy activation in the CRC cells was through MLH1/SIRT1/LC3 axis. To our knowledge, this is the first study to demonstrate that the DNA damage induces a cytoprotective molecular interaction between MLH1/SIRT1 and LC3 in CRC cells.

In conclusion, our results support the MLH1-dependent model of DNA damage-induced nucleophagy in CRC to overcome the cytotoxic stress by recycling the damaged nuclear components for cellular homeostasis and survival of the cancer cells. Therefore, we suggest that MLH1 mediates the LC3 and SIRT1 overexpression in these cancer cells. Consequently, the MLH1/SIRT1/LC3 axis may represent a potential and novel therapeutic target in CRC to overcome anticancer drug resistance.

Declarations

Author Contributions: Conceptualization, J.S.M., S.M., and M.S.A; methodology, J.S.M., and S.M.; formal analysis, S.M.; investigation, S.M.; resources, J.S.M., S.M., and M.S.A; data curation, S.M.; writing—original draft preparation, S.M. and J.S.M.; writing—review and editing, J.S.M., M.S.A, Q.H., and A.A.M; supervision, J.S.M. and A.A.M; project administration, J.S.M., and S.M.; funding acquisition, J.S.M., S.M., and M.S.A. All authors have read and agreed to the published version of the manuscript.

Funding: J.S.M is funded by the "Research Institute of Medical and Health Sciences (RIMHS), University of Sharjah (UOS), grant number 1901090159. M.S.A is funded by grants from RIMHS, UOS (1801090141-P) and Mohamed Bin-Rashid University (MBRU)-AlMahmeed Collaborative Research Award (ALM1914). S.M. is supported by grants from LABCO and UOS School of Graduate studies (Ph.D. thesis support P20). The funders had no role in the study's design, in the collection, analyses, or interpretation of data, in the writing of the manuscript, or in the decision to publish the results.

Institutional Review Board Statement: Not applicable.

Declaration of Competing Interest

The authors declare no conflict of interest

Acknowledgments

The authors wish to acknowledge the generous support of the Research Institute of Medical and Health Sciences, University of Sharjah, UAE.

Availability of data and material

All the relevant data is included with the manuscript.

Supplementary materials

Supplementary material associated with this article can be found, in the online version, at doi:10.1016/j.neo.2021.12.003.

References

1. Zamer Abi, AW B, Hamad M, Maghazachi AA, Muhammad JS. Genetic mutations and non-coding RNA-based epigenetic alterations mediating the warburg effect in colorectal carcinogenesis. *Biology* 2021;**10**(9):847.

2. Araghi M, Soerjomataram I, Jenkins M, Brierley J, Morris E, Bray F, et al. Global trends in colorectal cancer mortality: projections to the year 2035. *Int J Cancer* 2019;**144**(12):2992–3000 Epub 2018/12/12PubMed PMID: 30536395. doi:10.1002/ijc.32055.
3. Sinicrope FA, Foster NR, Thibodeau SN, Marsoni S, Monges G, Labianca R, et al. DNA mismatch repair status and colon cancer recurrence and survival in clinical trials of 5-fluorouracil-based adjuvant therapy. *J Natl Cancer Inst* 2011;**103**(11):863–75 Epub 2011/05/21PubMed PMID: 21597022; PubMed Central PMCID: PMC3110173. doi:10.1093/jnci/djr153.
4. Zeinalian M, Hashemzadeh-Chaleshtori M, Salehi R, Emami MH. Clinical aspects of microsatellite instability testing in colorectal cancer. *Adv Biomed Res* 2018;**7**:28 Epub 2018/03/14PubMed PMID: 29531926; PubMed Central PMCID: PMC5841008. doi:10.4103/abr.abr_185_16.
5. Schmoll HJ, Van Cutsem E, Stein A, Valentini V, Glimelius B, Haustermans K, et al. ESMO Consensus Guidelines for management of patients with colon and rectal cancer. a personalized approach to clinical decision making. *Ann Oncol: Off J Eur Soc Med Oncol* 2012;**23**(10):2479–516 Epub 2012/09/27PubMed PMID: 23012255. doi:10.1093/annonc/mds236.
6. Li GM. Mechanisms and functions of DNA mismatch repair. *Cell Res* 2008;**18**(1):85–98 Epub 2007/12/25PubMed PMID: 18157157. doi:10.1038/cr.2007.115.
7. Chen J, Sadowski I. Identification of the mismatch repair genes PMS2 and MLH1 as p53 target genes by using serial analysis of binding elements. *PNAS* 2005;**102**(13):4813–18 Epub 2005/03/23PubMed PMID: 15781865; PubMed Central PMCID: PMC555698. doi:10.1073/pnas.0407069102.
8. Levine B, Kroemer G. Biological functions of autophagy genes: a disease perspective. *Cell* 2019;**176**(1-2):11–42 Epub 2019/01/12PubMed PMID: 30633901; PubMed Central PMCID: PMC6347410. doi:10.1016/j.cell.2018.09.048.
9. Slobodnyuk K, Radic N, Ivanova S, Llado A, Trempolec N, Zorzano A, et al. Autophagy-induced senescence is regulated by p38alpha signaling. *Cell Death Dis* 2019;**10**(6):376 Epub 2019/05/17PubMed PMID: 31092814; PubMed Central PMCID: PMC6520338. doi:10.1038/s41419-019-1607-0.
10. Muhammad JS, Guimei M, Jayakumar MN, Shafarin J, Janeeh AS, AbuJabal R, et al. Estrogen-induced hypomethylation and overexpression of YAP1 facilitate breast cancer cell growth and survival. *Neoplasia* 2021;**23**(1):68–79 Epub 2020/11/27PubMed PMID: 33242831; PubMed Central PMCID: PMCPMC7695929. doi:10.1016/j.neo.2020.11.002.
11. Berg KCG, Eide PW, Eilertsen IA, Johannessen B, Bruun J, Danielsen SA, et al. Multi-omics of 34 colorectal cancer cell lines - a resource for biomedical studies. *Mol Cancer* 2017;**16**(1):116 Epub 2017/07/08. doi: 10.1186/s12943-017-0691-y. PubMed PMID: 28683746; PubMed Central PMCID: PMC5498998.
12. Li X, Zhou Y, Li Y, Yang L, Ma Y, Peng X, et al. Autophagy: A novel mechanism of chemoresistance in cancers. *Biomed Pharmacother* 2019;**119**:109415 Epub 2019/09/13PubMed PMID: 31514065. doi:10.1016/j.biopha.2019.109415.
13. Li Y, Jiang X, Zhang Y, Gao Z, Liu Y, Hu J, et al. Nuclear accumulation of UBC9 contributes to SUMOylation of lamin A/C and nucleophagy in response to DNA damage. *J Exp Clin Cancer Res* 2019;**38**(1):67 Epub 2019/02/13PubMed PMID: 30744690; PubMed Central PMCID: PMC6371487. doi:10.1186/s13046-019-1048-8.
14. Gruosso T, Mieulet V, Cardon M, Bourachot B, Kieffer Y, Devun F, et al. Chronic oxidative stress promotes H2AX protein degradation and enhances chemosensitivity in breast cancer patients. *EMBO Mol Med* 2016;**8**(5):527–49 Epub 2016/03/24PubMed PMID: 27006338; PubMed Central PMCID: PMCPMC5123617. doi:10.15252/emmm.201505891.
15. Meador JA, Zhao M, Su Y, Narayan G, Geard CR, Balajee AS. Histone H2AX is a critical factor for cellular protection against DNA alkylating agents. *Oncogene* 2008;**27**(43):5662–71 Epub 2008/06/11PubMed PMID: 18542054. doi:10.1038/onc.2008.187.
16. Zhao E, Hou J, Ke X, Abbas MN, Kausar S, Zhang L, et al. The roles of Sirtuin family proteins in cancer progression. *Cancers* 2019;**11**(12) Epub 2019/12/11PubMed PMID: 31817470; PubMed Central PMCID: PMC6966446. doi:10.3390/cancers11121949.
17. Huang R, Xu Y, Wan W, Shou X, Qian J, You Z, et al. Deacetylation of nuclear LC3 drives autophagy initiation under starvation. *Mol Cell* 2015;**57**(3):456–66 Epub 2015/01/21PubMed PMID: 25601754. doi:10.1016/j.molcel.2014.12.013.
18. Papandreou ME, Tavernarakis N. Nucleophagy: from homeostasis to disease. Cell death and differentiation. 2019;26(4):630-9. Epub 2019/01/17. doi: 10.1038/s41418-018-0266-5. PubMed PMID: 30647432; PubMed Central PMCID: PMC6460388.
19. Mijaljica D, Devenish RJ. Nucleophagy at a glance. *J Cell Sci* 2013;**126**(Pt 19):4325–30 Epub 2013/09/10PubMed PMID: 24013549. doi:10.1242/jcs.133090.
20. Burke B, Stewart CL. The nuclear Lamins: flexibility in function. *Nat Rev Mol Cell Biol* 2013;**14**(1):13–24 Epub 2012/12/06PubMed PMID: 23212477. doi:10.1038/nrm3488.
21. Yun CW, Lee SH. The roles of autophagy in cancer. *Int J Mol Sci* 2018;**19**(11) Epub 2018/11/08PubMed PMID: 30400561; PubMed Central PMCID: PMC6274804. doi:10.3390/ijms19113466.
22. Dou Z, Ivanov A, Adams PD, Berger SL. Mammalian autophagy degrades nuclear constituents in response to tumorigenic stress. *Autophagy* 2016;**12**(8):1416–17 Epub 2015/12/15PubMed PMID: 26654219; PubMed Central PMCID: PMC4968220. doi:10.1080/15548627.2015.1127465.
23. Hinrichsen I, Ernst BP, Nuber F, Passmann S, Schafer D, Steinke V, et al. Reduced migration of MLH1 deficient colon cancer cells depends on SPTAN1. *Mol Cancer* 2014;**13**:11 Epub 2014/01/25PubMed PMID: 24456667; PubMed Central PMCID: PMC3904401. doi:10.1186/1476-4598-13-11.
24. Ackermann A, Schrecker C, Bon D, Friedrichs N, Bankov K, Wild P, et al. Downregulation of SPTAN1 is related to MLH1 deficiency and metastasis in colorectal cancer. *PLoS One* 2019;**14**(3):e0213411 Epub 2019/03/12PubMed PMID: 30856214; PubMed Central PMCID: PMC6411122. doi:10.1371/journal.pone.0213411.
25. Glick D, Barth S, Macleod KF. Autophagy: cellular and molecular mechanisms. *J Pathol* 2010;**221**(1):3–12 Epub 2010/03/13PubMed PMID: 20225336; PubMed Central PMCID: PMC2990190. doi:10.1002/path.2697.
26. Luo G, Jian Z, Zhu Y, Chen B, Ma R, Tang F, et al. Sirt1 promotes autophagy and inhibits apoptosis to protect cardiomyocytes from hypoxic stress. *Int J Mol Med* 2019;**43**(5):2033–43 Epub 2019/03/14PubMed PMID: 30864731; PubMed Central PMCID: PMC6443335. doi:10.3892/ijmm.2019.4125.
27. Dou Z, Xu C, Donahue G, Shimi T, Pan JA, Zhu J, et al. Autophagy mediates degradation of nuclear lamina. *Nature* 2015;**527**(7576):105–9 Epub 2015/11/03PubMed PMID: 26524528; PubMed Central PMCID: PMC4824414. doi:10.1038/nature15548.